Available online at www.sciencedirect.com
ScienceDirect
Phytochemistry 69 (2008) 348–355
PHYTOCHEMISTRY
www.elsevier.com/locate/phytochem

Role of Tyr residues on the protein surface of cationic cell-wall-peroxidase (CWPO-C) from poplar: Potential oxidation sites for oxidative polymerization of lignin

Shinya Sasaki, Daisuke Nonaka, Hiroyuki Wariishi, Yuji Tsutsumi *, Ryuichiro Kondo

Department of Forest and Forest Products Sciences, Kyushu University, 6-10-1, Hakozaki, Higashiku, Fukuoka 812-8581, Japan

Received 25 October 2006; received in revised form 9 July 2007
Available online 29 October 2007

Abstract

It was previously reported that an unique peroxidase isoenzyme, cationic cell-wall-bound peroxidase (CWPO-C), from poplar callus oxidizes sinapyl alcohol, ferrocytochrome *c* and synthetic lignin polymers, unlike other plant peroxidases. Here, the catalytic mechanism of CWPO-C was investigated using chemical modification and homology modeling. The simulated CWPO-C structure predicts that the entrance to the heme pocket of CWPO-C is the same size as those of other plant peroxidases, suggesting that ferrocytochrome *c* and synthetic lignin polymers cannot interact with the heme of CWPO-C. Since Trp and Tyr residues are redox-active, such residues located on the protein surface were predicted to be active sites for CWPO-C. Modification of CWPO-C Trp residues did not suppress its oxidation activities toward guaiacol and syringaldazine. On the other hand, modification of CWPO-C Tyr residues using tetranitromethane strongly suppressed its oxidation activities toward syringaldazine and 2,6-dimethoxyphenol by 90%, respectively, and also suppressed its guaiacol oxidation activity to a lesser extent. Ferrocytochrome *c* was not oxidized by Tyr-modified CWPO-C. These results indicate that the Tyr residues in CWPO-C mediate its oxidation of syringyl compounds and high-molecular-weight substrates. Homology modeling indicates that Tyr-177 and Tyr-74 are located near the heme and exposed on the protein surface of CWPO-C. These results suggest that Tyr residues on the protein surface are considered to be important for the oxidation activities of CWPO-C with a wide range of substrates, and potentially unique oxidation sites for the plant peroxidase family.

Keywords: Poplar; *Poplus alba*; Salicaceae; Homology modeling; Lignin biosynthesis; Long-range electron transfer; Plant peroxidase; Tetranitromethane

1. Introduction

Lignin is a polymer of phenylpropanoid units with a variety of carbon–carbon and carbon–oxygen linkages, resulting in a complex structure. The final step of monolignol oxidation leading to lignin biosynthesis is catalyzed by plant peroxidases (Blee et al., 2003). Horseradish peroxidase (HRP) is a typical plant peroxidase that has been used to attempt to study the mechanism of monolignol dehydrogenative polymerization leading to lignins, even though HRP is not present in tissues that lignify to any extent (Syrjanen and Brunow, 1998, 2000). Angiosperm lignins consist of guaiacyl and syringyl units. HRP C and A2 oxidize coniferyl alcohol **1** efficiently, but not sinapyl alcohol **2** (Nielsen et al., 2001). *Arabidopsis thaliana* peroxidase A2 (ATP A2; 95% identity with HRP A2) was previously purified and cloned from a suspension culture of *A. thaliana* (Østergaard et al., 1996). Analysis of the substrate-binding mode of mature ATP A2 by docking simulation with three monolignols (*p*-coumaryl **3**, coniferyl **1** and sinapyl **2** alcohols) (Fig. 1) indicated that coniferyl **1** and *p*-coumaryl **3** alcohols bind well to the substrate-binding site of ATP A2 (Østergaard et al., 2000). On the other hand, sinapyl alcohol **2** did not bind to the substrate-binding site of ATP A2, since its 5-methoxy group overlapped with

* Corresponding author. Tel./fax: +81 92 642 4282.
E-mail address: y-tsutsu@agr.kyushu-u.ac.jp (Y. Tsutsumi).

0031-9422/$ - see front matter © 2007 Elsevier Ltd. All rights reserved.
doi:10.1016/j.phytochem.2007.08.020

Pro-139 (Østergaard et al., 2000). This prediction was suggested to be generally applicable, since Pro-139 is highly conserved in the majority of plant peroxidases. For example, 69 of 73 peroxidases in *A. thaliana* contain Pro-139 (Nielsen et al., 2001; Welinder et al., 2002). Since HRP and ATP A2 share high identity including Pro-139, HRP can be used as a representative of plant peroxidases that cannot utilize sinapyl alcohol **2** as a preferred substrate.

An unique peroxidase isoenzyme from poplar callus, cationic cell-wall-bound peroxidase (CWPO-C), has broad substrate versatility and was reported to use sinapyl alcohol **2** and syringaldazine **6** as preferred substrates (Tsutsumi et al., 1994, 1998; Aoyama et al., 2002; Sasaki et al., 2004). Furthermore, CWPO-C catalyzes the oxidation of synthetic lignin polymers and ferrocytochrome *c*, unlike other plant peroxidases (Sasaki et al., 2004). These observations suggest that the oxidation mechanism of CWPO-C is quite different from those of other plant peroxidases and appears to be required for lignin formation in plant cell walls.

Ferrocytochrome *c* is a 13-kDa heme protein that is larger than the entrance of the substrate access channels of peroxidases. However, fungal lignin peroxidase (LiP) can directly oxidize ferrocytochrome *c* (Wariishi et al., 1994). The Trp-171 residue located on the LiP surface was determined to be an oxidation site for its substrates (Blodig et al., 1998; Doyle et al., 1998; Johjima et al., 1999). These findings allowed us to postulate that either the oxidation site of CWPO-C is located on the protein surface, or that the entrance of the substrate access channel of CWPO-C is larger than those of other plant peroxidases.

In the present study, *in vitro* chemical modification techniques with *N*-bromosuccinimide (NBS) and tetranitromethane (TNM) were used to determine the key catalytic amino acid residues of CWPO-C. These were used since NBS can be employed for selective oxidation of exposed Trp residues to oxindolealanine (Blodig et al., 1998; Spande and Witkop, 1967), while TNM converts Tyr residues to 3-nitrotyrosine and has been used to assess the roles of Tyr residues in protein functions (Landfear et al., 1978; Miki and Wariishi, 2005). In addition to *in vitro* experiments, *in silico* homology modeling was employed to investigate the entrance size of the substrate access channel and determine the oxidation sites of CWPO-C.

2. Results and discussion

2.1. No definitive differences between the heme environment of CWPO-C and those of other plant peroxidases

A full-length CWPO-C cDNA was cloned using RT-PCR and RACE-PCR techniques. The predicted CWPO-C amino acid sequence contains a putative signal peptide (22 amino acids) at its *N*-terminus (Sasaki et al., 2006). The M_w and *p*I of the deduced amino acid sequence of the mature CWPO-C were calculated to be 32.3 kDa and 8.06, respectively. The molecular weight of the purified CWPO-C was previously determined to be approximately 32 kDa by SDS-PAGE (Tsutsumi et al., 1994).

An alignment analysis indicated that the catalytic sites of CWPO-C, including Arg-39, His-43, Pro-135 and His-165, were identical to those of ATP A2, HRP C and other plant peroxidases (Fig. 2) (Welinder, 1992). CWPO-C showed absorption maxima at 402 (Soret band), 496 and 635 nm, suggesting that it is a high-spin ferric peroxidase (Fig. 3a) (Tamura et al., 1972). The conserved functionally important amino acid residues and absorption spectrum of the CWPO-C also indicated that the heme environment of CWPO-C was identical to those of other plant peroxidases.

The simulated CWPO-C structure constructed by the Molecular Operating Environment (MOE) program predicts that the entrance to the heme pocket of CWPO-C is of the same size as those of the plant peroxidases HRP C and ATP A2 (Supplementary Figure). It was reported that binding of sinapyl alcohol **2** is sterically hindered in the ATP A2 peroxidase and other plant peroxidases due to overlap of the methoxyl group on the syringyl aromatic ring and Pro-139 (Østergaard et al., 2000). Our alignment analysis indicated that CWPO-C has a conserved Pro-135, which corresponds to Pro-139 in the other plant peroxidases (Fig. 2). Since ferrocytochrome *c* and syringyl

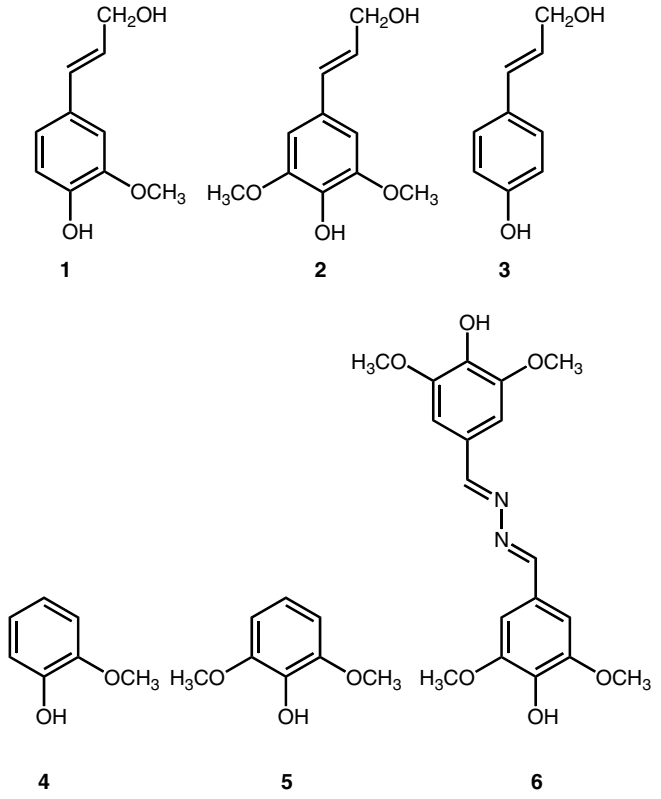

Fig. 1. Chemical structures of monolignols and substrates used for peroxidase assay. Monolignols, **1**: coniferyl alcohol; **2**: sinapyl alcohol; **3**: *p*-coumaryl alcohol. Substrates for peroxidase assay, **4**: guaiacol; **5**: 2,6-dimethoxyphenol; **6**: syringaldazine.

```
CWPO-C      1 -------MSQKVVLMFLLVAMAGTATVQGQGTRVGFYATTCRRAESIVRATVQSHFTSDS     53
HRPC        1 ----------------------------MQLTPTFYDNSCPNVSNIVRDTIVNELRSDP     31
HRPA2       1 -----------------------------QLNATFYSGTCPNASAIVRSTIQQAFQSDT     30
ATPA2       1 MAVTNLPTCDGLFIISLIVIVSSIFGTSSAQLNATFYSGTCPNASAIVRSTIQQALQSDT     60
                                          ..  .**  .*.... *** *..    **
CWPO-C     53 SIAPGLLRMHFHDCFVNGCDASILIDGANT---EKTAGPNLL-LRGYDVIADAKTQLEAE    109
HRPC       31 RIAASILRLHFHDCFVNGCDASILLDNTTSFRTEKDAFGNANSARGFPVIDRMKAAVESA     91
HRPA2      30 RIGASLIRLHFHDCFVDGCDASILLDDSGSIQSEKNAGPNANSARGFNVVDNIKTALENT     90
ATPA2      60 RIGASLIRLHFHDCFVNGCDASILLDDTGSIQSEKNAGPNVNSARGFNVVDNIKTALENA    120
              .* ... *.*******.*******.*   .   ** *..* ...**. * .  *...*
CWPO-C    109 CPGVVSCADILALAARDSVVLTKGLTWPVPTGRRDG-RVSLASDTSNLPGFTDSVDVQKQ    168
HRPC       91 CPRTVSCADLLTIAAQQSVTLAGGPSWRVPLGRRDSLQAFLDLANANLPAPFFTLPQLKD    151
HRPA2      90 CPGVVSCSDILALASEASVSLTGGPSWTVLLGRRDSLTANLAGANSAIPSPFEGLSNITS    150
ATPA2     120 CPGVVSCSDVLALASEASVSLAGGPSWTVLLGRRDSLTANLAGANSSIPSPIESLSNITF    180
              **..*** * *..*   ** * .*..* * .****.. . *. ...  * .   .
CWPO-C    168 KFAAFGLN-AQDLVTLVGGHTIGTTACQFFRYRLYNFTTTGNGADPSINPSFVSQLQTLC    227
HRPC      151 SFRNVGLNRSSDLVALSGGHTFGKNQCRFIMDRLYNFSNTGL-PDPTLNTTYLQTLRGLC    210
HRPA2     150 KFSAVGLN-TNDLVALSGAHTFGRARCGVFNNRLFNFSGTNG-PDPTLNSTLLSSLQQLC    208
ATPA2     180 KFSAVGLN-TNDLVALSGAHTFGRARCGVFNNRLFNFSGTGN-PDPTLNSTLLSTLQQLC    238
             .* ..***   ***.*.* **.*   *   .  ** **. *.  .**..* . .. *. **
CWPO-C    227 PQNGDGSRRIALDTGSQNSFDSSFFANLRSGQGILESDQKLWTDATTRTFVQRFLGVRGL    287
HRPC      210 PLNGNLSALVDFDLRTPTIFDNKYYVNLEEQKGLIQSDQELFSSPNATDTIPLVRSFANS    270
HRPA2     208 PQNGSASTITNLDLSTPDAFDNNYFANLQSNNGLLQSDQELFSTLGSA-TIAVVTSFASN    267
ATPA2     238 PQNGSASTITNLDLSTPDAFDNNYFANLQSNDGLLQSDQELFSTTGSS-TIAIVTSFASN    297
              *.**  *    .*. ..  **. ...** .  *...***.*..      ..  . ...
CWPO-C    287 AGLTFGVEFGRSMVKMSNIGVKTGTTGEIRRVCSAIN---                        324
HRPC      270 TQTFFNA-FVEAMDRMGNITPLTGTQGQIRLNCRVVNSNS                        309
HRPA2     267 QTLFFQA-FAQSMINMGNISPLTGSNGEIRLDCKKVDGS-                        305
ATPA2     297 QTLFFQA-FAQSMINMGNISPLTGSNGEIRLDCKKVNGS-                        335
                ..* . *  .*  *.** ..**  *.**. *  ..
```

Fig. 2. Alignment of the plant peroxidases ATP A2, HRP A2, HRP C and CWPO-C. Conserved amino acid residues in the catalytic sites are shown in blue. Tyr-74 and Tyr-177 are shown in red. Pro-139 (Pro-135 in the case of CWPO-C) is indicated in green. The name of each sequence corresponds to the deduced protein of the following GenBank DNA accession numbers: CWPO-C: AB210901; HRP C: J05552; ATP A2: X99952; HRP A2: P80679.

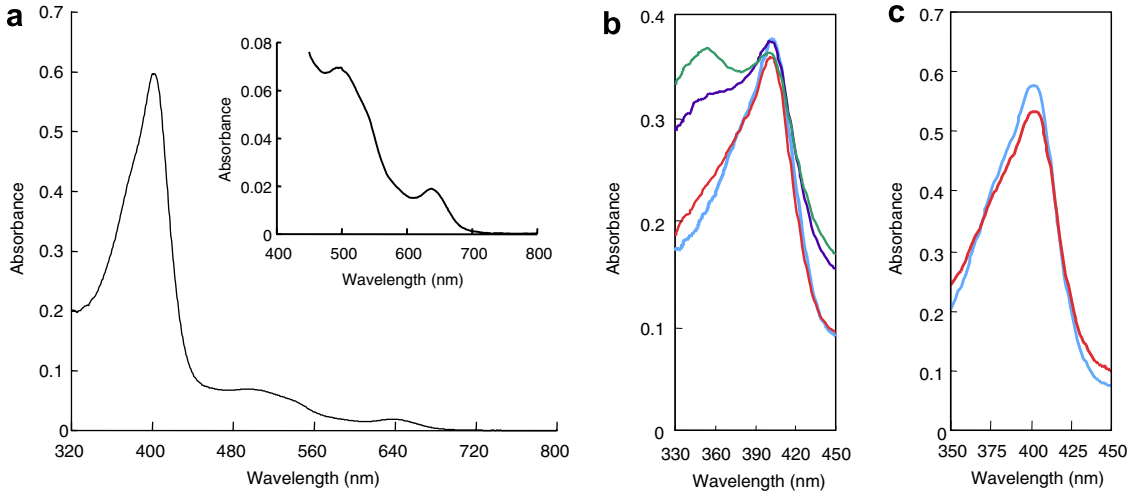

Fig. 3. Spectral changes of CWPO-C and HRP during TNM modification. (a) Absorption spectrum of native CWPO-C. Inset is a magnified view of the visible region of the spectrum. The spectrum was recorded in 50 mM Tris–HCl buffer (pH 7.5) containing 0.6 M NaCl. (b) Spectra of CWPO-C modified by 60 mM TNM. Light-blue: untreated control; red: 3-min treatment; purple: 10-min treatment; green: 30-min treatment. (c) Spectra of HRP modified by 60 mM TNM. Light-blue: untreated control; red: 30-min treatment.

compounds, including sinapyl alcohol **2**, cannot fit into the heme pocket of CWPO-C, a possible explanation was invoked for the unusually broad substrate versatility of CWPO-C, namely that the oxidation sites for the substrates were located on the protein surface. Such exposed oxidation sites would allow the enzyme to interact with a wide range of substrates, including syringyl compounds, lignin polymers and ferrocytochrome *c*.

2.2. Tyr residues on the protein surface as oxidation sites for syringyl compounds and high-molecular-weight substrates

Tyr and Trp residues are known to be redox-active and advantageous as electron transfer mediators. Prostaglandin H synthase was found to have a radical center in a tyrosine residue (Tyr-385) near the heme (Smith et al., 1992). Several other reports have indicated that Tyr radicals are formed in the reactions between cytochrome *c* peroxidase mutants and catalase peroxidase (Musah and Goodin, 1997; Zhang et al., 2002; Zhao et al., 2004). The Trp-171 residue on LiP has also been postulated as an oxidation site (Blodig et al., 1998; Doyle et al., 1998; Johjima et al., 1999).

In the present study, chemical modifications of Tyr with TNM and Trp residues with NBS were employed to determine which residues represent oxidation sites in CWPO-C. By the NBS modification, the activities of CWPO-C and HRP were barely altered and >95% of the activities were retained (Table 1). This indicates that Trp residues in CWPO-C do not act as substrate oxidation sites.

Following TNM modification, changes in the absorption spectra of CWPO-C were observed. During TNM modification, the absorbance at 350 nm due to Tyr nitration increased with increasing reaction time (Fig. 3b) (Sokolovsky et al., 1967). On the other hand, absorbance changes at 350 nm were almost negligible for HRP (Fig. 3c). These results show that Tyr nitration only occurs in CWPO-C. TNM-modified CWPO-C lost 67% of its guaiacol **4** oxidation activity following a 30-min treatment, whereas TNM-modified HRP only lost 20% of its guaiacol **4** oxidation activity following the same treatment (Fig. 4a). The remarkable decrease in the guaiacol **4** oxidation activity of CWPO-C along with its increased absorbance at 350 nm indicates that Tyr modification decreases the oxidation activity of CWPO-C. These results suggest that Tyr residues play crucial roles in the oxidation of substrates by CWPO-C. In the case of HRP, the observed decrease in guaiacol **4** oxidation activity (20%) after TNM treatment was nearly consistent with the decrease in Soret (402 nm) absorption (~15%), indicating that the decreased guaiacol **4** oxidation activity was due to heme bleaching caused by reactive oxygen species produced during the TNM treatment (Wariishi and Gold, 1989, 1990). In control experiments, we determined whether 6% ethanol in water added to the reaction mixture affected peroxidase activity, since this represents the same volume of ethanol added to the reaction mixtures with TNM. The peroxidase activities of CWPO-C and HRP were not decreased in the control experiments (data not shown).

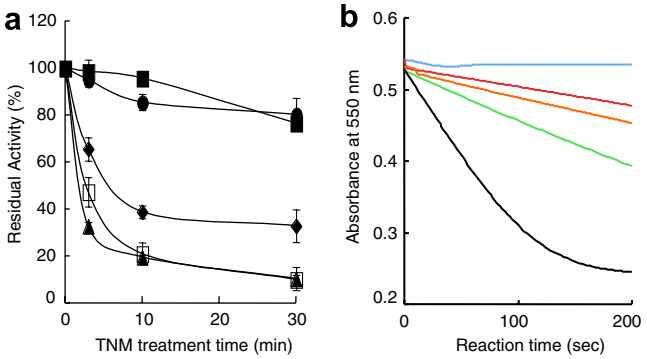

Fig. 4. Effects of TNM modification on the oxidations of various compounds by CWPO-C and HRP. (a) Effects of TNM modification of CWPO-C and HRP on the oxidations of guaiacol **4**, 2,6-DMP **5** and syringaldazine **6**. ■: Guaiacol **4** (HRP); ●: syringaldazine **6** (HRP); ◆: guaiacol **4** (CWPO-C); ▲: syringaldazine **6** (CWPO-C); □: 2,6-DMP **5** (CWPO-C). (b) Oxidation of ferrocytochrome *c* by TNM-treated and untreated CWPO-C. Decreases in the absorbance at 550 nm, indicating oxidation of ferrocytochrome *c*, were monitored. Blue: spontaneous oxidation; red: H_2O_2; black: untreated CWPO-C and H_2O_2; green: 3-min treated CWPO-C and H_2O_2; orange: 30-min treated CWPO-C and H_2O_2.

The effects of TNM modification on the oxidation activities toward guaiacol **4** and syringyl substrates were compared. Guaiacol **4** was used as a model guaiacyl compound, while 2,6-dimethoxyphenol **5** (2,6-DMP) and syringaldazine **6** were used as representative syringyl compounds (Fig. 1). TNM–CWPO-C lost 90% of its syringaldazine **6** oxidation activity after a 30-min treatment, while the guaiacol **4** oxidation activity was retained at about 33% (Fig. 4a). These results suggest that TNM modification of CWPO-C has a stronger effect on its activity toward syringyl compounds than toward guaiacyl compounds. Next, a similar decrease in 2,6-DMP **5** oxidation activity to that in the syringaldazine **6** oxidation activity was confirmed (Fig. 4a). Syringyl compounds, including 2,6-DMP **5** and syringaldazine **6**, are not predicted to bind in the heme pocket of plant peroxidases (Østergaard et al., 2000). On the other hand, guaiacol **4** fits well into the heme pocket (Henriksen et al., 1999). These results indicate that syringyl compounds are oxidized by Tyr residues exposed

Table 1
Peroxidase activities of NBS-modified CWPO-C and HRP

Time (min)	NBS-CWPO-C		NBS-HRP	
	Sy	Gu	Sy	Gu
0	55,000 ± 1000 (100)	10,100 ± 200 (100)	3610 ± 70 (100)	14,800 ± 1000 (100)
3	57,400 ± 3800 (104)	11,300 ± 400 (111)	3830 ± 100 (106)	15,300 ± 400 (104)
10	53,400 ± 3500 (99)	10,200 ± 400 (101)	3600 ± 100 (99)	14,400 ± 1200 (97)
30	58,700 ± 900 (107)	11,500 ± 500 (113)	3600 ± 300 (99)	13,800 ± 800 (93)

Note: Oxidation velocities were expressed as reaction product in μmol/min/mg protein.
Relative activities were given in parentheses. Sy: syringaldazine oxidizing activity; Gu: guaiacol oxidizing activity.

on the protein surface of CWPO-C, while guaiacyl compounds are oxidized at two sites, in the heme pocket and at Tyr residues on the protein surface.

In addition to the oxidation of monomeric compounds, the oxidation activity toward ferrocytochrome *c* was examined. As shown in Fig. 4b, CWPO-C oxidized ferrocytochrome *c* rapidly, whereas no extensive decrease in the absorbance was observed in the reaction with TMN-modified CWPO-C after 30 min. It was obvious that ferrocytochrome *c* could not bind to the heme pocket of the peroxidase. These results strongly support the hypothesis that large substrates unable to bind to the heme pocket of CWPO-C are oxidized by Tyr residues located on the protein surface.

2.3. Prediction of the oxidation sites of CWPO-C

CWPO-C contains four Tyr residues (Tyr-8, Tyr-74, Tyr-177 and Tyr-180). CWPO-C and HRP share two Tyr residues, Tyr-8 and Tyr-180. During TNM modification of both peroxidases, nitration of Tyr residues was clearly observed for CWPO-C by the increased absorbance at 350 nm, whereas nitration of the Tyr residues in HRP did not occur. This represents convincing evidence that Tyr-8 and Tyr-180 are not nitrated by TNM, and suggests that Tyr-74 and/or Tyr-177 become nitrated in CWPO-C.

We tried to identify the nitrated Tyr residues by peptide mass fingerprint analysis (PMF) with MALDI-TOF-MS. However, the ions of mononitrated target peptides, including Tyr residues (Tyr-74 and Tyr-177) of TNM-modified CWPO-C, were not detected by MALDI-TOF-MS analysis, whereas the ions of nine other peptides were detected in the same sample (matched peptide number: 9; sequence coverage: 54.5%) (Supplementary Table). Similarly, the ions of non-modified target peptides, including Tyr residues (Tyr-74 and Tyr-177) of non-modified CWPO-C, were not detected (Supplementary Table).

Homology modeling indicated that Tyr-8 is buried in the CWPO-C protein (Fig. 5). Tyr-180 is conserved among CWPO-C and other general plant peroxidases, such as HRP, and located at a distance of 20 Å from the heme (Figs. 2 and 5). The distances of Tyr-74 and Tyr-177 from the heme edge are 14 and 11 Å, respectively. Both of these residues are found on the protein surface (Fig. 5). Distances of <14 Å have been reported to be appropriate for long-range electron transfer with the heme edge (Choinowski et al., 1999; Musah and Goodin, 1997; Zhang et al., 2002; Zhao et al., 2004). In the case of fungal lignin peroxidase (LiP), site-directed mutations of Trp-171 were introduced in LiP H8, and it was shown that the variant enzymes were unable to oxidize veratryl alcohol (Doyle et al., 1998; Gelpke et al., 2002). Recently, compound I of the HRP F179Y mutant was shown to form a radical on Tyr-179 and catalyze the oxidation of 3,3′5,5′-tetramethylbenzidine (Ichimura et al., 2005). Tyr-179 of this HRP mutant is located on the protein surface and its geometry is similar to that of Tyr-177 of CWPO-C. This finding supports the premise that Tyr-177 of CWPO-C is a possible oxidation site. Some plant peroxidase isoenzymes have also been reported to oxidize sinapyl alcohol **2** as their preferred substrate (Gabaldón et al., 2005; Barceló and Pomar, 2001; Marjamaa et al., 2006), similar to CWPO-C. ZePrx34.70 and ZePrx33.44 purified from *Zinnia elegans* were found to utilize sinapyl alcohol **2** as their best substrate among three monolignols (*p*-coumaryl **3**, coniferyl **1** and sinapyl **2** alcohols) examined (Gabaldón et al., 2005). More

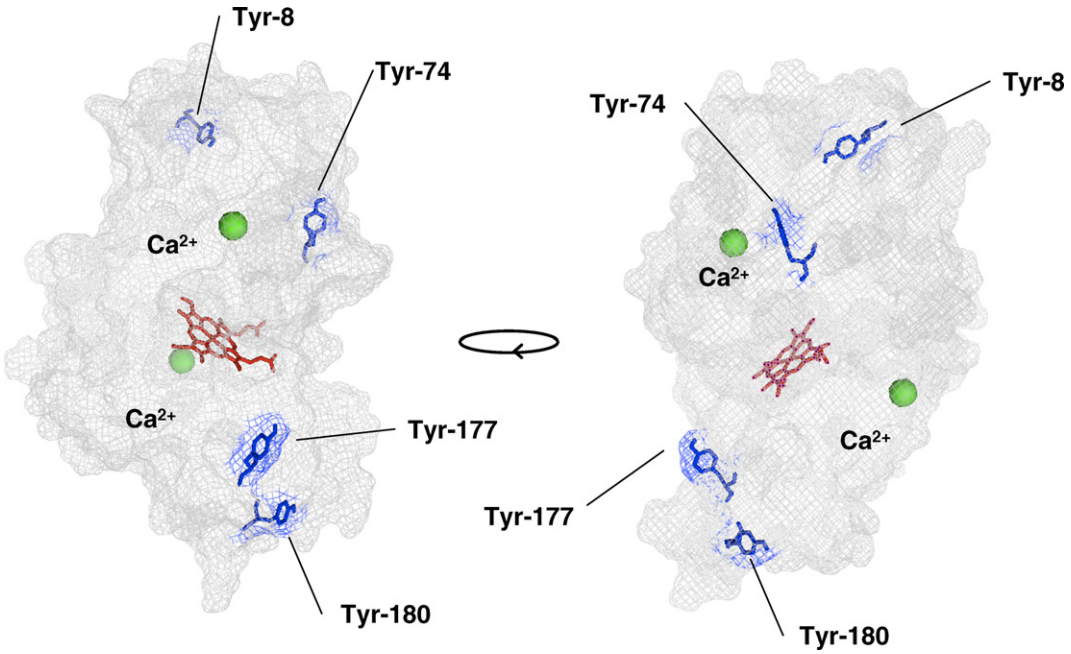

Fig. 5. Locations of the four Tyr residues in CWPO-C. Tyr-177 and Tyr-74 are located near the heme and exposed on the protein surface.

recently, BPX1 purified from *Betula pendula* was shown to oxidize sinapyl alcohol **2** more effectively than coniferyl alcohol **1** (Marjamaa et al., 2006). Concerning the deduced amino acid sequences of ZePrx34.70 and ZePrx33.44, they contain Tyr-74 but not Tyr-177. Other Tyr residues (Tyr-7, Tyr-180, Tyr-222, Tyr-223 and Tyr-252) in ZePrx34.70 and ZePrx33.44 are assumed to be distant from the heme (>20 Å) or buried in the protein. Therefore, Tyr-74 may be an important residue in sinapyl alcohol **2** oxidation by ZePrx34.70 and ZePrx33.44. Regarding these results, Tyr-74 and/or Tyr-177 of CWPO-C are possible oxidation sites for the oxidation of syringyl and high-molecular-weight compounds.

2.4. Concluding remarks: impact of protein surface Tyr residues as potential oxidation sites for lignin polymerization

With respect to the physiological roles of CWPO-C, Tyr residues located on its surface could easily interact with lignin polymers. Based on the "End-wise" polymerization process, monolignol radicals could be coupled to the growing-polymer in order to produce a lignin macromolecule (Sarkanen, 1971). CWPO-C polymerizes sinapyl alcohol oligomers and sinapyl alcohol **2**, producing a polymer of greater molecular weight, whereas HPR produces sinapyl alcohol dimers rather than catalyzing polymerization (Aoyama et al., 2002). CWPO-C is able to directly catalyze the oxidation of synthetic lignin dehydropolymerisates (Sasaki et al., 2004). Histochemical analysis of CWPO-C in poplar stems indicated that CWPO-C is mainly located at the cell corners and in the intercellular layer, consistent with lignin deposition in the developing xylem of poplar stem (Sasaki et al., 2006). The localization profile supports that CWPO-C is a plausible peroxidase isoenzyme involved in lignification (Sasaki et al., 2006). Based on previous reports and the present study, we propose that Tyr residues located on the protein surface of CWPO-C potentially represent unique oxidation sites for monolignol oxidation during dehydrogenative polymerization leading to lignin(s).

3. Experimental

3.1. Plant materials and chemicals

Poplar (*Populus alba* L.) callus was induced on Murashige and Skoog basal medium supplemented with 3% sucrose, 1.0 mg l^{-1} 2,4-dichlorophenoxyacetic acid, 0.5 mg l^{-1} kinetin and 0.8% agar, and maintained on this medium at 25 °C in the dark. CWPO-C was purified from the poplar callus as described previously (Aoyama et al., 2002). HRP type VI was purchased from Sigma–Aldrich (St. Louis, MO) and used without further purification. Ferrocytochrome *c* was prepared from ferricytochrome *c* as described previously (Wariishi et al., 1994). Protein contents were determined using a protein assay kit (Bio-Rad, Richmond, CA) with bovine serum albumin (BSA) as the protein standard. Poplar trees (*P. alba*) grown in Kyushu University were used for CWPO-C cloning. TNM was purchased from Sigma–Aldrich. NBS, guaiacol **4**, 2,6-DMP **5** and syringaldazine **6** were purchased from Wako Pure Chemicals Industries Ltd. (Tokyo, Japan).

3.2. Homology modeling of CWPO-C

A CWPO-C cDNA was cloned using RT-PCR and RACE-PCR techniques as described in our previous paper (Sasaki et al., 2006). Homology modeling of CWPO-C was performed using the MOE program (Chemical Computer Group Inc.). The ATP A2 crystal structure (protein data bank entry 1pa2) (Østergaard et al., 2000) was selected as the most appropriate template, since CWPO-C shares the highest amino acid sequence identity (45%) with ATP A2 among the peroxidases whose crystal structures have been reported. After modeling and energy minimization, 10 intermediate models were generated and subjected to coarse energy minimization using the AMBER89 force field. Among the intermediates, the most suitable model selected by MOE (packing score, −2.251) was applied to subsequent revision and full energy minimization. Next, full energy minimization was run by the Engh–Huber force field. Finally, a CWPO-C model with good geometry (root mean square deviation of C topology, 0.008) was obtained. All modeling and energy minimization steps were carried out under an environment including the heme imported from the template. The obtained tertiary model of CWPO-C was output as a pdb file, and subsequently visualized and analyzed using the Pymol program (DeLano, 2002).

3.3. Chemical modification of peroxidases

A TNM stock solution (1 M) in ethanol–H_2O_2 (95:5, v/v) was prepared. The reaction mixture (20 μl) comprised 5.0 μM CWPO-C or HRP and 60 mM TNM in 50 mM Tris–HCl buffer (pH 7.5) containing 0.6 M NaCl. After incubation at 25 °C for 3, 10 or 30 min, the reaction mixture was diluted by 25-fold. Excess TNM was removed using a Centricon (10,000 cut-off; Millipore, Billerica, MA), and the modified products were used without further purification. For control experiments, ethanol (1.2 μl) was added to the reaction mixture instead of the TNM stock solution.

NBS was recrystallized from water. An NBS stock solution (5 mM) in 50 mM Tris–HCl buffer (pH 7.5) containing 0.6 M NaCl was prepared immediately prior to use. NBS modification was performed as previously described (Johjima et al., 2002) with slight modifications. The reaction mixture (20 μl) comprised 1.0 μM CWPO-C or HRP and 50 μM NBS in 50 mM Tris–HCl buffer (pH 7.5) containing 0.6 M NaCl. After incubation at 25 °C for 3, 10 or 30 min, the reaction mixture was diluted by 25-fold. Excess NBS was removed using the above-described Centricon and

the modified products were used without further purification.

3.4. Assay for peroxidase activity

Peroxidase activity was assayed using guaiacol **4** and syringaldazine **6** as substrates as described previously (Tsutsumi and Sakai, 1994). The oxidations of guaiacol **4** and syringaldazine **6** were monitored spectrophotometrically at 470 and 530 nm, respectively ($\varepsilon_{470} = 5570\ M^{-1}\,cm^{-1}$ and $\varepsilon_{530} = 6500\ M^{-1}\,cm^{-1}$). The 2,6-DMP **5** oxidation activity was measured based on oxidative dimerization of 2,6-DMP **5** ($\varepsilon_{469} = 49{,}600\ M^{-1}\,cm^{-1}$) (Wariishi et al., 1992). All reactions were performed at 30 °C in 50 mM Tris–HCl buffer (pH 7.5) containing 0.6 M NaCl. The enzyme activity determined for each substrate was expressed as μmol of reaction product per mg protein per min.

For ferrocytochrome *c* oxidation, the reaction mixture (1 ml) comprised 20 μM ferrocytochrome *c*, 2.3 μg of CWPO-C or TNM-treated CWPO-C and 10 μM H_2O_2 in 50 mM Tris–HCl buffer (pH 7.5) containing 0.6 M NaCl. The reaction was initiated by adding the H_2O_2 and carried out at 30 °C. The absorbance decreases at 550 nm, indicating oxidation of ferrocytochrome *c*, were monitored at 30 °C (Margoliash and Frohwirt, 1959).

3.5. Peptide mass fingerprint analysis

Aliquots (3.2 μg) of 30-min TNM-modified CWPO-C and non-modified CWPO-C were subjected to SDS-PAGE. The target bands were excised from the gel after Coomassie Blue staining, and digested with trypsin. The resulting tryptic digests were applied to Voyager DE MALDI-TOF-MS target plates, and the peptide ions were detected by MALDI-TOF-MS (Voyager DE, Applied Biosystems, Foster City, CA) as previously described (Shimizu et al., 2005).

Acknowledgments

We are grateful to Dr. Y. Miki (Kyushu University) for valuable discussions regarding the TNM modification, and to Professor K. Ishimori (Hokkaido University) for helpful discussions on the F179Y HRP mutant. This work was supported by Grants-in-Aid for Scientific Research from the Ministry of Education, Culture, Sports, Science and Technology of Japan (Nos. 15380121 and 17-6161).

Appendix A. Supplementary data

Supplementary data associated with this article can be found, in the online version, at doi:10.1016/j.phytochem.2007.08.020.

References

Aoyama, W., Sasaki, S., Matsumura, S., Hirai, H., Tsutsumi, Y., Nishida, T., 2002. Sinapyl alcohol-specific peroxidase isoenzyme catalyzes the formation of the dehydrogenative polymer from sinapyl alcohol. J. Wood Sci. 48, 497–504.

Barceló, A.R., Pomar, F., 2001. Oxidation of cinnamyl alcohols and aldehydes by a basic peroxidase from lignifying *Zinnia elegans* hypocotyls. Phytochemistry 57, 1105–1113.

Blee, K.A., Choi, J.W., O'Connell, A.P., Schuch, W., Lewis, N.G., Bolwell, G.P., 2003. A lignin-specific peroxidase in tobacco whose antisense suppression leads to vascular tissue modification. Phytochemistry 64, 163–176.

Blodig, W., Doyle, W., Smith, A.T., Piontek, K., 1998. Autocatalytic formation of a hydroxy group at Cβ of Trp171 in lignin peroxidase. Biochemistry 37, 8832–8838.

Choinowski, T., Blodig, W., Winterhalter, K.H., Piontek, K., 1999. The crystal structure of lignin peroxidase at 1.70 Å resolution reveals a hydroxy group on the cbeta of tryptophan 171: a novel radical site formed during the redox cycle. J. Mol. Biol. 286, 809–827.

DeLano, W.L.T., 2002. The PyMOL Molecular Graphics System. USA DeLano Scientific, San Carlos, CA.

Doyle, W.A., Blodig, W., Veitch, N.C., Piontek, K., Smith, A.T., 1998. Two substrate interaction sites in lignin peroxidase revealed by site-directed mutagenesis. Biochemistry 37, 15097–15105.

Gabaldón, C., López-Serrano, M., Pedreño, M.A., Barceló, A.R., 2005. Cloning and molecular characterization of the basic peroxidase isoenzyme from *Zinnia elegans*, an enzyme involved in lignin biosynthesis. Plant Physiol. 139, 1138–1154.

Gelpke, M.D.S., Lee, J., Gold, M.H., 2002. Lignin peroxidase oxidation of veratryl alcohol: Effects of the mutants H82A, Q222A, W171A, and F267L. Biochemistry 41, 3498–3506.

Henriksen, A., Smith, A.T., Gajhede, M., 1999. The structures of the horseradish peroxidase C-ferulic acid complex and the ternary complex with cyanide suggest how peroxidases oxidize small phenolic substrates. J. Biol. Chem. 274, 35005–35011.

Ichimura, S., Yugihara, Y., Teramoto, M., Takahashi, S., Morishima, I., Ishimori, K., 2005. Regulation of radical center and substrate specificity in horseradish peroxidase. In: Abstract of Seventh International Peroxidase Symposium, p. 41.

Johjima, T., Itoh, N., Kabuto, M., Tokimura, F., Nakagawa, T., Wariishi, H., Tanaka, H., 1999. Direct interaction of lignin and lignin peroxidase from *Phanerochaete chrysosporium*. Proc. Natl. Acad. Sci. USA 96, 1989–1994.

Johjima, T., Wariishi, H., Tanaka, H., 2002. Veratryl alcohol binding sites of lignin peroxidase from *Phanerochaete chrysosporium*. J. Mol. Catal. B 17, 49–57.

Landfear, S.M., Lipscomb, W.N., Evans, D.R., 1978. Functional modifications of aspartate transcarbamylase induced by nitration with tetranitromethane. J. Biol. Chem. 253, 3988–3996.

Margoliash, E., Frohwirt, N., 1959. Spectrum of horse-heart cytochrome *c*. Biochemistry 71, 570–572.

Marjamaa, K., Kukkola, E., Lundell, T., Karhunen, P., Saranpää, P., Fagerstedt, K.V., 2006. Monolignol oxidation by xylem peroxidase isoforms of Norway spruce (*Picea abies*) and silver birch (*Betula pendula*). Tree Physiol. 26, 605–611.

Miki, Y., Wariishi, H., 2005. Characterization of lignin peroxidase from *Trametes cervina*: Determination of oxidation site and catalytic mechanism. In: Abstract of Seventh International Peroxidase Symposium, p. 43.

Musah, R.A., Goodin, D.B., 1997. Introduction of novel substrate oxidation into cytochrome *c* peroxidase by cavity complementation: oxidation of 2-aminothiazole and covalent modification of the enzyme. Biochemistry 36, 11665–11674.

Nielsen, K.L., Indiani, C., Henriksen, A., Feis, A., Becucci, M., Gajhede, M., Smulevich, G., Welinder, K.G., 2001. Differential activity and structure of highly similar peroxidases. Spectroscopic, crystallo-

graphic, and enzymatic analyses of lignifying *Arabidopsis thaliana* peroxidase A2 and horseradish peroxidase A2. Biochemistry 40, 11013–11021.

Østergaard, L., Abelskov, A.K., Mattsson, O., Welinder, K.G., 1996. Structure and organ specificity of an anionic peroxidase from *Arabidopsis thaliana* cell suspension culture. FEBS Lett. 98, 243–247.

Østergaard, L., Teilum, K., Mirza, O., Mattsson, O., Petersen, M., Welinder, K.G., Mundy, J., Gajhede, M., Henriksen, A., 2000. Arabidopsis ATP A2 peroxidase. Expression and high-resolution structure of a plant peroxidase with implications for lignification. Plant Mol. Biol. 44, 231–243.

Sarkanen, K.V., 1971. Precursors and their polymerization. In: Sarkanen, K.V., Ludwig, C.H. (Eds.), Lignins. Wiley-Interscience, New York, pp. 95–163.

Sasaki, S., Nishida, T., Tsutsumi, Y., Kondo, R., 2004. Lignin dehydrogenative polymerization mechanism: a poplar cell wall peroxidase directly oxidizes polymer lignin and produces in vitro dehydrogenative polymer rich in β-O-4 linkage. FEBS Lett. 562, 197–201.

Sasaki, S., Baba, K., Nishida, T., Tsutsumi, Y., Kondo, R., 2006. The cationic cell-wall-peroxidase having oxidation ability for polymeric substrate participates in the late stage of lignification of *Populus alba* L. Plant Mol. Biol. 62, 797–807.

Shimizu, M., Yuda, N., Nakamura, T., Tanaka, H., Wariishi, H., 2005. Metabolic regulation at the tricarboxylic acid and glyoxylate cycles of the lignin-degrading basidiomycete *Phanerochaete chrysosporium* against exogenous addition of vanillin. Proteomics 5, 3919–3931.

Smith, W.L., Eling, T.E., Kulmacz, R.J., Marnett, L.J., Tsai, A.L., 1992. Tyrosyl radicals and their role in hydroperoxide-dependent activation and inactivation of prostaglandin endoperoxide synthase. Biochemistry 31, 3–7.

Sokolovsky, M., Riordan, J.F., Vallee, B.L., 1967. Tetranitromethane. A reagent for the nitration of tyrosyl residues in proteins. Biochemistry 5, 3582–3589.

Spande, T.F., Witkop, B., 1967. In: Hirs, C.H.W. (Ed.), Methods in Enzymology, vol. XI. Academic Press, New York, p. 498.

Syrjanen, K., Brunow, G., 1998. Oxidative cross coupling of *p*-hydroxycinnamic alcohols with dimeric arylglycerol–aryl ether lignin model compounds: the effect of oxidation potentials. J. Chem. Soc., Perkin Trans. I 1, 3425–3429.

Syrjanen, K., Brunow, G., 2000. Regioselectivity in lignin biosynthesis: the influence of dimerization and cross-coupling. J. Chem. Soc., Perkin Trans. I 1, 183–187.

Tamura, M., Asakura, T., Yonetani, T., 1972. Heme-modification studies on horseradish peroxidase. Biochim. Biophys. Acta 268, 292–304.

Tsutsumi, Y., Sakai, K., 1994. Lignin biosynthesis in woody angiosperm tissue II. Peroxidase related to syringyl and guaiacyl lignin biosynthesis in *Populus* callus cultures. Mokuzai Gakkaishi 40, 744–750.

Tsutsumi, Y., Nishida, T., Sakai, K., 1994. Lignin biosynthesis in woody angiosperm tissue III. Isolation of substrate-specific peroxidase related to the dehydrogenative polymerization of sinapyl and coniferyl alcohols from *Populus* callus cultures. Mokuzai Gakkaishi 40, 1348–1354.

Tsutsumi, Y., Matsui, K., Sakai, K., 1998. Substrate-specific peroxidases in woody angiosperms and gymnosperm participate in regulating the dehydrogenative polymerization of syringyl and guaiacyl type lignins. Holzforschung 52, 275–281.

Wariishi, H., Gold, M.H., 1989. Lignin peroxidase compound III: formation, inactivation, and conversion to the native enzyme. FEBS Lett. 243, 165–168.

Wariishi, H., Gold, M.H., 1990. Lignin peroxidase compound III. Mechanism of formation and decomposition. J. Biol. Chem. 265, 2070–2077.

Wariishi, H., Valli, K., Gold, M.H., 1992. Manganese (II) oxidation by manganese peroxidase from the basidiomycete *Phanerochaete chrysosporium*. Kinetic mechanism and role of chelators. J. Biol. Chem. 267, 23688–23695.

Wariishi, H., Sheng, D., Gold, M.H., 1994. Oxidation of ferrocytochrome *c* by lignin peroxidase. Biochemistry 33, 5545–5552.

Welinder, K.G., 1992. Peroxidases: structure–function relationship. In: Penel, C., Gaspar, T., Greppin, H. (Eds.), Plant Peroxidases 1980–1990. University of Geneva, Switzerland, pp. 1–24.

Welinder, K.G., Justesen, A.F., Kjærsgård, I.V., Jensen, R.B., Rasmussen, S.K., Jespersen, H.M., Duroux, L., 2002. Structural diversity and transcription of class III peroxidases from *Arabidopsis thaliana*. Eur. J. Biochem. 269, 6063–6081.

Zhang, H., He, S., Mauk, A.G., 2002. Radical formation at Tyr39 and Tyr153 following reaction of yeast cytochrome *c* peroxidase with hydrogen peroxide. Biochemistry 41, 13507–13513.

Zhao, X., Girotto, S., Yu, S., Magliozzo, R.S., 2004. Evidence for radical formation at Tyr-353 in *Mycobacterium tuberculosis* catalase-peroxidase (KatG). J. Biol. Chem. 279, 7606–7612.